ChemComm

Accepted Manuscript

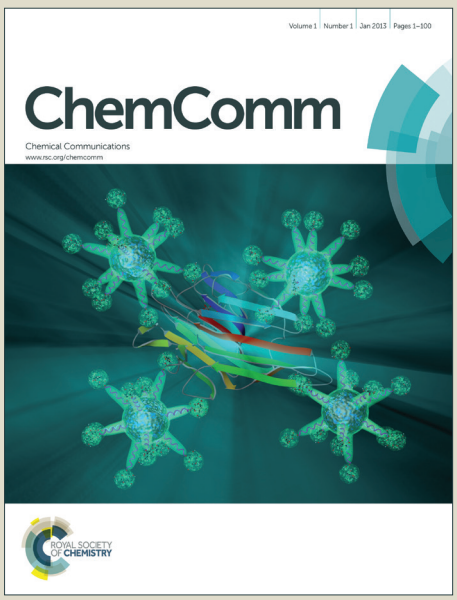

ROYAL SOCIETY OF CHEMISTRY

www.rsc.org/chemcomm

Cite this: DOI: 10.1039/c0xx00000x

www.rsc.org/xxxxxx

COMMUNICATION

pH-Responsive Self-Assembly of Fluorophore-Ended Homopolymers

Jin Zhang,[a] Shusen You,[a] Shouke Yan,[a] Klaus Müllen,[b] Wantai Yang,[a] Meizhen Yin*[a]

Received (in XXX, XXX) Xth XXXXXXXXX 20XX, Accepted Xth XXXXXXXXX 20XX
DOI: 10.1039/b000000x

pH-responsive perylene-ended amphiphilic homopolymers can self-assemble into flower-like structures by pH-adjustment. Both the π–π stack of perylene end groups and electrostatic repulsion effect of the polymer chains contribute to the pH-responsive self-assembly in aqueous solution.

Perylene derivatives are key chromophores with high chemical and photochemical stability, high molar absorptivity, and high fluorescence quantum yields.[1] They readily form regular self-assemblies in organic solvents due to strong π-π interaction provided by the benzene rings. This self-assembling behavior in organic solvents and the applications of the self-assemblies has been studied intensively.[2] Recently, Zang's group reported the well-defined one-dimensional self-assemblies of *N,N'*-di(propanoic acid)-perylene-3,4,9,10-tetracarboxylic diimide (PDI-PA) in aqueous solutions by pH triggered hydrogelation.[3] Unlike PDIs, perylene-3,4-dicarboxylic acid monoimides (PMIs) have asymmetric structures at the imide positions. The self-assembly behaviors of asymmetric PMIs are studied, but only on small molecular level.[4] The self-assembly of PMI-ended macromolecule has not been reported yet. Therefore, it is of high interest to prepare PMIs-based polymers and investigate their self-assembly behavior.

Small-molecule amphiphilies (surfactants and lipids) and amphiphilic block copolymers have been studied for many years because they can form a variety of self-assembled aggregates, such as spheres, rods, vesicles, lamellae, and worm-like structures.[5] Particularly, stimuli-responsive or smart block copolymers have aroused great interest in their self-assembling behavior. By changing the solution environment, the copolymers can be tuned between double-hydrophilic (double-hydrophobic) and amphiphilic; thus, the self-assemblies are sensitive to the surroundings, such as the pH value, temperature, and pressure.[6] Recently, aimed at simplifying the synthesis route of polymers and providing nanoparticles with new structures, the self-assemblies of homopolymers have been studied. The self-assembly behavior of styrene-based amphiphilic homopolymer was first reported by Arumugam et al.[7] Du's group introduced a series of self-assemblies with different reversible addition-fragmentation chain transfer (RAFT) end groups and demonstrated that a small amount of hydrophobic end-groups significantly affected the self-assembly behavior of the homopolymers.[8]

In this communication, we reported two PMI-ended polymers (**P1** and **P2**, **Scheme 1**) bearing primary amines and their pH-responsive self-assemblies. The fluorophore PMI moiety provides a large rigid hydrophobic surface, whereas the flexible poly(amino ethyl methacrylate) (polyAEMA) behaves as a pH-sensitive hydrophilic moiety. The fluorophore-ended amphiphilic homopolymer, fabricated into pH-sensitive flower-like structure, is the first example of PMI-ended amphiphilic homopolymer with pH-responsive self-assembly that is caused by the π–π stacking of hydrophobic PMI moieties and the electrostatic repulsion of the weak polyelectrolyte polyAEMA.

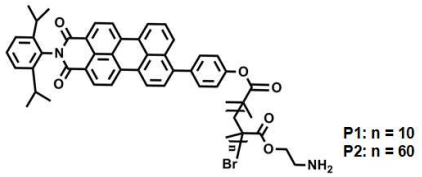

Scheme 1 Chemical structures of **P1** and **P2**

P1 and **P2** were synthesized by atom transfer radical polymerization (ATRP) followed by the removal of protective groups. PolyAEMA is a weak polyelectrolyte and its pKa value has been reported to be about pH 8.[9] In order to study the effect of electrostatic repulsion on the assemblies, we designed and synthesized PMI-based polyAEMA with short (**P1**) and long (**P2**) repeating unit. PMI is a typical fluorophore with the absorption peak around 500 nm **(Fig. S3, ESI†)**.[10] The UV-vis spectra of **P1** and **P2** were monitored at various pH values (**Fig. 1**). As the pH values increase from 2 to 12, the maximum absorption peak around 500 nm decreases gradually because of the protonation of polyAEMA under acid conditions. This decrease is accompanied by the appearance of a new absorption peak at 550 nm in the spectra of **P1** and **P2**, and this observation is attributed to the π-π stacking state of perylene derivatives.[11] The UV-vis spectra indicate the pH-responsive aggregation of both **P1** and **P2** in aqueous solution and this inspired us to investigate the self-assembly behaviors of **P1** and **P2** after the solvent evaporation.

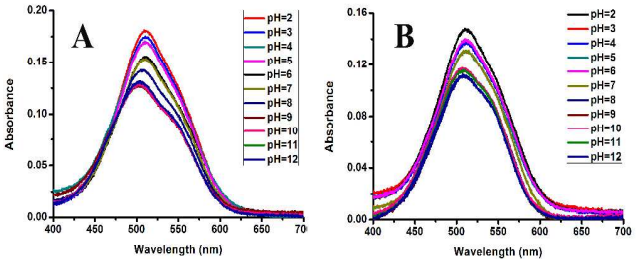

Fig. 1 pH-dependent UV-vis absorption spectra of (A) **P1** and (B) **P2** molecularly dissolved in tris-HCl buffers over a pH range of 2-12, the concentration is 3×10^{-5} M.

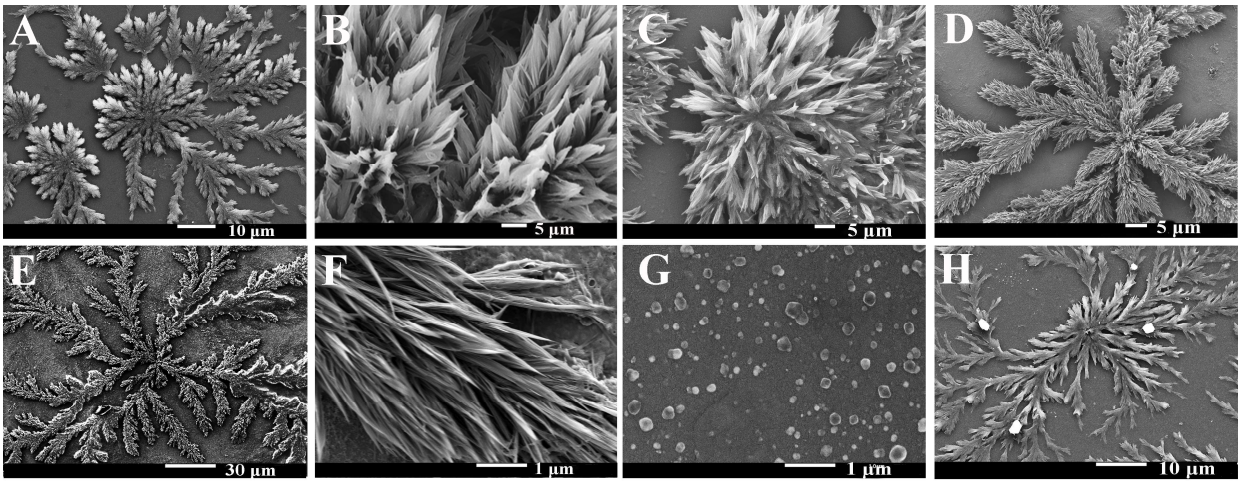

Fig. 2 Self-assemblies of **P1**: (A) pH=12 (>pKa), (C) pH=8 (=pKa) and (D) pH=2 (<pKa). Self-assemblies of **P2**: (E) pH=12 (>pKa), (G) pH=8 (=pKa). (B) and (F) are the magnified views of (A) and (E), respectively. The concentration is 3×10^{-5} M. (H) Recovered assemblies of **P2** by treating acidic solution of polymer with alkali.

The morphologies of the PMI-ended amphiphilic homopolymers **P1** and **P2** were investigated at various pH values on the surface of silica by scanning electron microscopy (SEM). Each polymer was first dissolved in water to form a homogeneous solution (3×10^{-3} M) and then diluted 100 times to form a solution with a given pH value. The sample was then placed under ambient conditions to allow the solvent to slowly evaporate for about 10 h. **Fig. 2** shows the morphologies of **P1** and **P2** under different pH conditions. The aggregations of **P1** (pH > pKa = pH 8) present leaf-like structures of 1.5 μm in length and about 700 nm in width (**Fig. 2A**, **2B**). The assembled flower-like structures of **P1** show inconspicuous changes upon pH adjustments over the range 12-2 (**Fig. 2A**, **2C**, **2D**). On the other hand, the flower-like structures of **P2** self-assemble only under alkaline conditions from pH 10 to pH 12 (**Fig. 2E**). **P2** transformes into sphere-type assemblies around pH 8 (**Fig. 2G**) and disaggregates under acidic conditions (pH 2 to pH 4, **Fig. S5**). The flower-like aggregates of **P2** at pH 12 are formed by the linkage of nanobelts with an average length of 4 μm and an average width of 250 nm (**Fig. 2F**). For comparison, the homopolymer polyAEMA without PMI end-group was also observed by SEM under the same conditions. **Fig. S6 (ESI†)** clearly shows a homogeneous film without any flower-like aggregates. The results indicate that the flower-like or sphere-like assemblies of PMI-ended amphiphilic homopolymers are induced by the π–π interactions of the hydrophobic PMI moieties.

Interestingly, the disaggregated structures of **P2** in acidic solution are recovered as flower-like assemblies by adding a small amount of NaOH solution (0.1M) (**Fig. 2H**). The observed small white crystals are NaCl, as confirmed by the blank experiment without homopolymer under the same conditions (**Fig. S7, ESI†**). These results indicate that the self-assembly behavior is influenced by the electrostatic repulsion of the weak polyelectrolyte. In acidic solution, the polymer chains are protonated and fully extended. **P2** bears long polyAEMA chains; thus, the electrostatic repulsion is stronger than the π–π interaction of PMI. As a result, the flower-like structures of **P2** are disaggregated by this strong electrostatic repulsion. Unlike those of **P2**, the flower-like structures of **P1** with short polyAEMA chains did not disaggregate at low pH values (**Fig. 2D**) because the electrostatic repulsion force is relatively low and can not disintegrate the assemblies. By alkalizing the solution to pH 8 (about the same as the pKa value), the polymer chains are partly deprotonated. Thus, **P2** aggregates into sphere-like structures due to the decline of the electrostatic repulsion effect (**Fig. 2G**). As the polymer chains are deprotonated at high pH values (pH > pKa, **Fig. 2A**), both **P1** and **P2** aggregate into flower-like structures because of the π–π stacking of PMI end-groups.

Laser light scatting (LLS) was used to further understand the morphology changes with pH variations. With increasing pH value of the solution, the hydrodynamic radius $\langle R_h \rangle$ of **P1** increases **(Table S2**, **ESI†)**. The results further demonstrate that the electrostatic repulsion force affects the self-assembly of **P1**, but can not disaggregate the self-assemblies, which is in agreement with the SEM results. **Table 1** gives the LLS results of **P2** at different pH values. The average radius of gyration ($\langle R_g \rangle$) and the weight-average molar mass of the microspheres ($M_{w,sphere}$) were determined by using a Zimm plot (**Fig. S8**, **ESI†**). The $\langle R_g \rangle/\langle R_h \rangle$ value can be used to characterize the morphology of the self-assemblies under different conditions.[12]

Table 1. DLS/SLS results of **P2** at different pH values

pH[a]	$\langle R_h \rangle$ (nm)	$\langle R_g \rangle$[b] (nm)	$\langle R_g \rangle/\langle R_h \rangle$	$M_{w,sphere}$ (g mol^{-1})	(N_{agg})[c]
2	41	84	2.04	1.6×10^8	7413
4	45	55	1.22	1.7×10^8	7870
8	60	47	0.78	1.8×10^8	8481
10	89	63	0.70	3.9×10^8	17727
12	100	66	0.66	4.1×10^8	18636

[a] The concentration of the homopolymer is 3×10^{-5} M.

[b] $R_g^2 = \int_v^\infty \rho(r)r^2 dv \Big/ \int_v^\infty \rho(r)dv$, where ρ(r) is the mass density at r.

[c] $N_{agg} = M_{w,sphere} \Big/ M_{w,polymer}$

For a normal Gaussian coil and a uniform solid sphere, the theoretical $\langle R_g \rangle/\langle R_h \rangle$ values are equal to 1.05-2.05 and 0.775, respectively. In the present case, the measured $\langle R_g \rangle/\langle R_h \rangle$ values

for **P2** at pH 2 and pH 4 are 2.04 and 1.22, respectively, which are close to the theoretical values for a Gaussian coil. As the pH increases to 8, the $\langle R_g \rangle / \langle R_h \rangle$ value decreases to 0.78, indicating that the sphere-like structures are solid spheres. As the pH further increases to 10, the molar mass ($M_{w,sphere}$) increases, indicating the aggregation of micelles.[13]

Scheme 2 illustrates the self-assembly behavior of **P2**. **P2** self-assembles into flower-like structures through three steps: (1) the amphiphilic homopolymer self-assembles into micelles at about the pKa value due to the π–π interaction of PMI, (2) the micelles aggregate at pH > pKa into nanobelts and nanoleaves, which subsequently conjugate into Y-junctions, and (3) upon solvent evaporation, the Y-junctions spread out from their root, acting as a branch to form flower-like structures.[14] In acid solution, the total protonation and full extension of the polymer chains greatly affect the self-assembly behavior. Thus, the polymer displays a normal Gaussian coil, which is stretched out in acidic solution. As the pH increases to around pKa value, the polymer chains are partly deprotonated. The decline of the electrostatic repulsion effect leads to the coiling of polymer chains, which indirectly influences the self-assembly of **P2**. Thus, **P2** self-assembles to micelles around the pKa value. As the solution is further alkalized (pH > pKa), the polymer chains become totally uncharged. With the disappearance of the electrostatic repulsion effect, the micelles get together. During solvent evaporation, the aggregated micelles are stacked to form flower-like structures. The tunable morphologies of the flower-like structures indicate the potential applications of the polymer in pH-sensitive nanodevices. In the case of **P1**, the π–π stacking of PMI moieties plays the main role in the self-assembly due to the short polyelectrolyte chains, thus, the assembled structures do not depend on the pH value. Therefore, the assembled approaches are well interpreted.

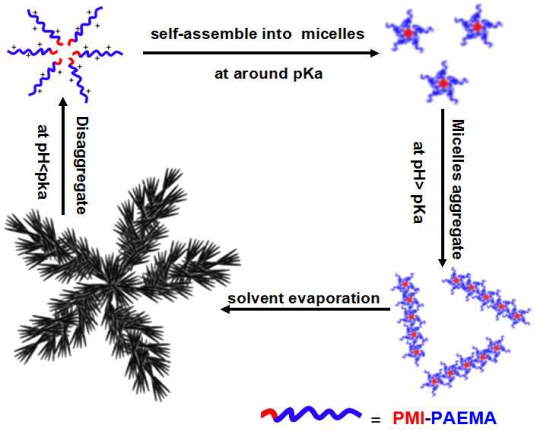

Scheme 2 Self-assembly of PMI-based amphiphilic homopolymer **P2** in response to pH variations.

In summary, the synthesis and self-assembly of two amphiphilic homopolymers (**P1**, **P2**) are reported. **P1** and **P2** are polymers with fluorophore PMI end group and polymer chains with different lengths. Due to electrostatic repulsion, the self-assemblies of **P2** with long polymer chains are pH-switchable. On the other hand, **P1** with short polymer chains shows inconspicuous changes with changes in pH. The effect of the electrostatic repulsion on the self-assembly is fully characterized by UV-vis spectroscopy, SEM, and DLS/SLS. The results provide an improved understanding of the nature of self-assembly involving the interaction between the π–π stacking of end-group moieties and pH-responsive polymers at the micrometer scale. This study provides not only a simple route to tune the morphology of PMI-ended homopolymer self-assemblies, but also the potential applications of PMI-ended homopolymer as a pH sensor in pH-sensitive nanodevices.

This work was financially supported by the National Science Foundation of China (21174012, 51103008 and 51221002), the Beijing Natural Science Foundation (2142026), and the New Century Excellent Talents Award Program from Ministry of Education of China (NCET-10-0215).

Notes and references

a State Key Laboratory of Chemical Resource Engineering, Key Laboratory of Carbon Fiber and Functional Polymers, Ministry of Education, Beijing University of Chemical Technology, 100029 Beijing, China, Email: yinmz@mail.buct.edu.cn
b Max-Planck-Institude for Polymer Reseach, Ackermannweg 10, 55128 Mainz, Germany.
† Electronic Supplementary Information (ESI) available: See DOI: 10.1039/b000000x/

1. (a) M. Yin, Z. Xu, B. He, J. Shen and W. Yang, *Chem. Commun.*, 2013, 49, 3646-3648; (b) S. Becker, A. Böhm and K. Müllen, *Chem-Eur. J.*, 2000, 6, 3984-3990; (c) M. Chen and M. Yin, *Prog. Polym. Sci.*, 2014, 39, 365-395; (d) B. He, Y. Chu, M. Yin, K. Müllen, C. An and J. Shen, *Adv. Mater.*, 2013, **25**, 4580-4584.
2. (a) K. Balakrishnan, A. Datar, R. Oitker, H. Chen, J. Zuo and L. Zang, *J. Am. Chem. Soc.*, 2005, **127**, 10496-10497; (b) Y. Che, A. Datar, K. Balakrishnan and L. Zang, *J. Am. Chem. Soc.*, 2007, **129,** 7234-7235; (c) J. Hu, W. Kuang, K. Deng, W. Zou, Y. Huang, Z. Wei and C. F. Faul, *Adv. Funct. Mater.*, 2012, **22**, 4149-4158.
3. A. Datar, K. Balakrishnan and L. Zang, *Chem. Comm.,* **49**, 6894-6896.
4. (a) J. M. Mativetsky, M. Kastler, R. C. Savage, D. Gentilini, M. Palma, W. Pisula, K. Müllen and P. Samori, *Adv. Funct. Mater.*, 2009, **19**, 2486-2494; (b) E. Fron, L. Puhl, I. Oesterling, C. Li, K. Müllen, F. C. De Schryver, J. Hofkens and T. Vosch, *Chem. Phys. Chem.*, 2011, **12**, 595-608
5. (a) B. M. Discher, Y.-Y. Won, D. S. Ege, J. C. Lee, F. S. Bates, D. E. Discher and D. A. Hammer, *Science*, 1999, **284**, 1143-1146; (b) H. Cui, Z. Chen, S. Zhong, K. L. Wooley and D. J. Pochan, *Science*, 2007, **317**, 647-650; (c) Z. Geng, S. Guan, H.-m. Jiang, Z.-w. Liu and L. Jiang, *Chin J Polym Sci*, 2014, **32**, 92-97.
6. (a) Du, J. Z.; Chen, Y. M. *Angew. Chem. Int. Ed.* 2004, **43**, 5084-5087; (b) Discher, D. E.; Eisenberg, A. *Science*, 2002, **297**, 967-973;(c) Blanazs, A.; Madsen, J.; Battaglia, G.; Ryan, A. J.; Armes, S. P, *J. Am. Chem. Soc.*, 2011, **133**, 16581-16587.
7. S. Arumugam, D. R. Vutukuri, S. Thayumanavan and V. Ramamurthy, *J. Am. Chem Soc*, 2005, **127**, 13200-13206.
8. (a) M. S. Lavine, *Science*, 2011, **333**, 386; (b) J. Du, H. Willcock, J. P. Patterson, I. Portman and R. K. O'Reilly, *Small*, 2011, **7**, 2070-2080.
9. S. You, Q. Cai, K. Müllen, W. Yang and M. Yin, *Chem. Commun.*, 2014, **50**, 823-825.
10. Y. Avlasevich, C. Li and K. Müllen, *J. Mater. Chem*, 2010, **20**, 3814-3826.
11. (a) Wurthner, F., *Chem. Commun.* , 2004, **14**, 1564; (b) Balakrishnan, K., Datar, A., Oitker, R., Chen, H., Zuo, J., Zang, L. *J. Am. Chem. Soc.* 2005, **127**, 10496-10499.
12. (a) W. Burchard, *Makromol. Chem., Macromol. Symp.*, 1988, **18**, 1; (b) M. Antonietti, W. Bremser and M. Schimidt, *Macromolecules*, 1990, **23**, 3796-3805.
13. Y. Hou, C. Yu, G. Liu, T. Ngai and G. Zhang, *J. Phys. Chem. B*, 2010, **114**, 3799-3803.
14. Y. Chen, Y. Feng, J. Gao and M. Bouvet, *J. Colloid Interface Sci.,* 2012, **368**, 387-394.